

# Macroscopic Treatment of Kinematic Waves in Traffic Flow Described by Intelligent Driver Model

Imperial College London

**Abstract**— We find numerical solutions to the simplified Intelligent Driver Model using the fourth-order Runge-Kutta method in NodeJS. We then use the simulation to model scenarios that induce compression and rarefaction traffic waves. Using Python and Mathematica, we analyse the output data from the simulation to calculate the macroscopic properties of traffic waves, including wave speed, amplitude and wavelength. We consider the effect of changing vehicle parameters on the stability of the IDM equation and offer possible further investigations.

## I. INTRODUCTION

THE study of traffic behaviour is central to managing and ensuring efficient flow of traffic. Many universities offer traffic and transport management courses. In developed countries, the ability to manage and adjust traffic flow according to external conditions is integral to road safety.

Scientists use traffic models to simulate the behaviour of vehicles for a given set of parameters. For example, the Lighthill-Whitham model<sup>[1]</sup> uses the continuity equation to study how the localised vehicle density propagates in a traffic jam. The Payne-Whitham model<sup>[2]</sup> hypothesises that the speed,  $u$ , of a vehicle at a position,  $x$ , is a function of the vehicle density,  $\rho$ , at that position (i.e.  $u = u(\rho(x))$ ) – this is an attempt to extract a microscopic description of vehicle behaviour by modelling macroscopic properties, such as vehicle density. Depending on the aims of the investigation, each model has its own uses and can provide insight into either the microscopic or macroscopic behaviour of vehicles in traffic jams.

## II. THEORY

### A. Intelligent Driver Model

For our investigation, we wish to observe how microscopic behaviour influences the macroscopic properties of a traffic wave. We use a simplified version of the Intelligent Driver Model (IDM), which is a mathematical model describing individual vehicle behaviour. Given  $N$  vehicles, the IDM is a set of  $N$  coupled second-order differential equations in position,  $x$ ,

which do not have analytic solutions and must be solved numerically. Each equation describes the acceleration of a single vehicle, which is coupled to the vehicle directly ahead. For the  $\alpha^{\text{th}}$  vehicle, the acceleration is,

$$\frac{dv_\alpha}{dt} = a_\alpha \left[ 1 - \left( \frac{v_\alpha}{v_0^{(\alpha)}} \right)^4 - \left( \frac{s^*(v_\alpha, \Delta v_\alpha)}{\Delta x_\alpha} \right)^2 \right] \quad (2.1)$$

where,

$$s^*(v_\alpha, \Delta v_\alpha) = s_0^{(\alpha)} + \max \left[ T_\alpha v_\alpha + \frac{v_\alpha \Delta v_\alpha}{2\sqrt{a_\alpha b_\alpha}}, 0 \right] \quad (2.2)$$

is the minimum desired gap to the vehicle ahead. The variable  $\Delta v_\alpha$  is the speed of the  $\alpha^{\text{th}}$  vehicle relative to the vehicle ahead (i.e. the approach speed) and  $\Delta x_\alpha$  is the separation between these two vehicles. The variables  $a_\alpha$ ,  $b_\alpha$ ,  $T_\alpha$ ,  $v_0^{(\alpha)}$  and  $s_0^{(\alpha)}$  are parameters describing the behaviour of the  $\alpha^{\text{th}}$  vehicle. The definitions of these parameters are given below.

Table I: A description of the parameters used in Eq. (2.1) and Eq. (2.2).

Symbol	Description
$a$	The maximum positive acceleration of the vehicle on a free road (i.e. no vehicle ahead). Note that this is not necessarily the maximum acceleration that the vehicle is capable of.
$b$	A positive value which characterises the desired deceleration of the vehicle. This is the rate at which a vehicle will decelerate if it is given sufficient time to decelerate at will.
$T$	The safe-time headway – this is the time that a driver allows themselves to react to changes in the behaviour of the vehicle ahead. This directly influences the desired separation that a driver will aim to maintain with the vehicle ahead while moving.
$v_0$	The desired velocity – this is the speed that a driver will maintain on a free road.
$s_0$	The jam distance – this is the separation that a driver will maintain with the vehicle ahead when in a stationary traffic jam.

### B. General Behaviour of IDM Equation

It may be more instructive to re-write Eq. (2.1) as,

$$\frac{dv_\alpha}{dt} = a_\alpha \left[ 1 - \left( \frac{v_\alpha}{v_0^{(\alpha)}} \right)^\delta \right] - a_\alpha \left( \frac{s^*(v_\alpha, \Delta v_\alpha)}{\Delta x_\alpha} \right)^2 \quad (2.3)$$

where  $\delta = 4$  is the *acceleration exponent*. The first term is the uncoupled acceleration due to a vehicle not travelling at its desired velocity and the latter term is the deceleration due to coupling with the vehicle ahead.

In the simple case of there being no leading vehicle (i.e. a free road), there is no coupling so the second term becomes negligible and Eq. (2.3) simplifies to,

$$\frac{dv_\alpha}{dt} = a_\alpha \left[ 1 - \left( \frac{v_\alpha}{v_0^{(\alpha)}} \right)^\delta \right] \quad (2.4)$$

This is bounded above by  $a_\alpha$  and hence the maximum positive acceleration of the vehicle is  $a_\alpha$ . However, the term is not bounded below and can therefore lead to extreme negative acceleration if  $v_\alpha \gg v_0^{(\alpha)}$  due to the exponent of  $\delta$ . The effect of the exponent should also be considered, so we attempt solutions to Eq. (2.4) for different values of  $\delta$ . Without loss of generality, we take  $a_\alpha = 1\text{ms}^{-2}$ ,  $b_\alpha = 1\text{ms}^{-1}$  and find numerical solutions for  $\delta = \{1, 4, 20\}$ .

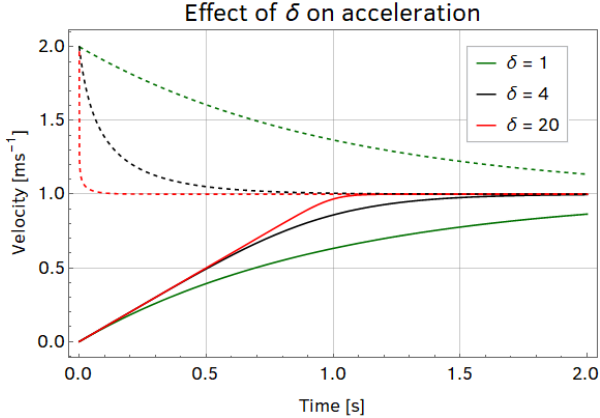


Figure 1<sup>[3]</sup>: Plot showing the effect of the acceleration exponent,  $\delta$ , on the acceleration of a vehicle from  $v_\alpha = 0\text{ms}^{-1}$  to  $v_0^{(\alpha)} = 1\text{ms}^{-1}$  (**solid line**) and deceleration from  $v_\alpha = 2\text{ms}^{-1}$  to  $v_0^{(\alpha)} = 1\text{ms}^{-1}$  (**dashed line**). Higher values of  $\delta$  lead to more sudden changes in the acceleration of the vehicle (i.e. the *jerk* is greater, which can be verified by differentiating Eq. (2.4) with respect to time). This is consistent with the behaviour of more aggressive drivers, who are likely to accelerate and decelerate sharply.

The brief<sup>[4]</sup> suggests  $\delta = 4$  as a realistic balance between the tendency of a vehicle to accelerate or decelerate to its desired speed and the rate at which it is able to do so. A more thorough analysis would consider the magnitude of the jerk experienced by a typical accelerating vehicle, but we choose to use  $\delta = 4$  for simplicity and reserve the option to edit this parameter later as necessary.

In the case  $v_\alpha = v_0^{(\alpha)}$ , Eq. (2.3) instead becomes,

$$\frac{dv_\alpha}{dt} = -a_\alpha \left( \frac{s^*(v_\alpha, \Delta v_\alpha)}{\Delta x_\alpha} \right)^2 \quad (2.5)$$

which is coupled to the behaviour of the vehicle ahead. For finite  $\Delta x_\alpha$ , this term is always negative and hence causes a deceleration. In the limit as  $\Delta x_\alpha \rightarrow \infty$  (i.e. a free road), the acceleration in Eq. (2.5) takes its smallest magnitude and is bounded above by  $dv_\alpha/dt \rightarrow 0$ . Similar to Eq. (2.4), the acceleration is unbounded below and can lead to extreme negative acceleration if  $s^* \gg \Delta x_\alpha$ .

The minimum desired gap term described in Eq. (2.2) characterises the gap that each driver aims to maintain with the vehicle ahead. This has a minimum value of  $s^* = s_0^{(\alpha)}$  when  $v_\alpha = 0$  referring to the case when the vehicle is stationary in a traffic jam. When  $v_\alpha > 0$ , the desired minimum gap is also dependent on the second term in  $s^*$ ,

$$\max \left[ T_\alpha v_\alpha + \frac{v_\alpha \Delta v_\alpha}{2\sqrt{a_\alpha b_\alpha}}, 0 \right] \quad (2.6)$$

which takes its minimum value of 0 when,

$$\Delta v_\alpha \leq -2T_\alpha \sqrt{a_\alpha b_\alpha} \quad (2.7)$$

This means that the approach rate is negative, so the vehicle ahead is travelling faster than the current vehicle.

In the case  $\Delta v_\alpha = 0$ , the expression in Eq. (2.6) simplifies to give  $s^* = s_0^{(\alpha)} + T_\alpha v_\alpha$ . The  $T_\alpha v_\alpha$  term is the *reaction distance* that would be travelled by the vehicle during the safe time headway interval.

If  $\Delta v_\alpha < 0$ , the approach rate is negative (i.e. the vehicle ahead is traveling faster so the gap between the two vehicles is increasing). Then from Eq. (2.2), the reaction distance is decreased by

$$\left| \frac{v_\alpha \Delta v_\alpha}{2\sqrt{a_\alpha b_\alpha}} \right| \quad (2.8)$$

since if the vehicle ahead is travelling faster, the driver will need less additional time to react to changes in the behaviour of the vehicle ahead. If  $\Delta v_\alpha > 0$ , the approach rate is positive so the gap between the two vehicles is decreasing. Then, the reaction distance is increased by the amount in Eq. (2.8).

### C. Deficiencies of IDM Equation

The Intelligent Driver Model is a mathematical model and is therefore constrained to work within a range of acceptable parameters and under certain assumptions or simplifications. Deviation from this range of validity may cause the equation to diverge or produce results which are unrealistic.

One assumption in the model is that each vehicle is a point-like particle. The reason for this is that vehicle length does not impact the outcome of the results. Factoring in vehicle length into Eq. (2.1) makes the simulation more realistic but is redundant because the dynamics of each vehicle are unchanged.

Another problem with the IDM equation is that it cannot be used to model stationary vehicles. Consider the  $v_\alpha/v_0^{(\alpha)}$  term in Eq. (2.1). Then, setting the desired velocity of a vehicle to  $v_0^{(\alpha)} = 0$  to model stationary vehicles causes the equation to diverge. This problem can be addressed by creating a *virtual vehicle* which abides by the equations  $v_\alpha = 0$  and  $dv_\alpha/dt = 0$ . These virtual vehicles behave as a traffic light and allow trailing vehicles to come to a stop behind the virtual vehicle.

We remarked on the unboundedness of Eq. (2.4) and Eq. (2.5) in the cases  $v_\alpha \gg v_0^{(\alpha)}$  and  $s^* \gg \Delta x_\alpha$ , respectively. These two cases cause an extreme negative acceleration and can produce unphysical results. A possible solution to this would be to set a lower bound on the acceleration that a vehicle can achieve. A further consequence of this unboundedness is that vehicles may achieve negative velocities (i.e. travel in reverse). This is a physically-acceptable but unrealistic result. It is unlikely that a vehicle in the real world would reverse if it was too close to the vehicle ahead. These extreme cases can be largely avoided by restricting the use of the IDM equation to slow-moving traffic so that the magnitude of acceleration is relatively small.

The model has no capability for detecting when a crash has occurred (i.e.  $\Delta x_\alpha < 0$ ). When time is discretised in numerical integration, it is possible for a trailing vehicle to overshoot the vehicle ahead between two time-steps, but the model would continue to produce valid results since the overshooting vehicle has jumped the queue and is now following a different vehicle, so  $\Delta x_\alpha > 0$  again. This can be avoided by fixing the order of the queue, so that if a vehicle jumps the queue then  $\Delta x_\alpha < 0$  and hence a crash can be detected.

The model can be used to produce a roundabout in which every vehicle is coupled. This would complicate the analysis of the results since multiple traffic waves would begin to interfere with each other in the circular loop. Instead, we model traffic as if it is on an infinite highway, with the leading vehicle exhibiting no coupling behaviour. Then, the coupled term in Eq. (2.3) is negligible, so the leading vehicle behaves according to Eq. (2.4).

#### D. Definitions

Firstly, we define  $\alpha$  as the index of a vehicle in the queue such that  $\alpha = 1$  represents the first vehicle and  $\alpha = 2,3,4\dots$  represent the subsequent trailing vehicles in order. We also define the *displacement*

of the  $\alpha^{\text{th}}$  vehicle,  $\Delta x_\alpha$ , as the distance to the vehicle ahead.

We define a *traffic wave* as a disturbance in the local vehicle density which propagates backwards through space. To quantitatively study traffic waves, we define the two types of wave-packets we expect to observe. A *rarefaction traffic wave-packet* is one where plotting the displacement of a given vehicle against time produces a curve whose stationary points are local maxima. Conversely, a *compression traffic wave-packet* is such that the displacement against time produces a curve whose stationary points are local minima.

A wave is defined as an oscillation of a quantity about an equilibrium position (e.g. displacement in transverse waves, density in longitudinal waves). We define the *initial equilibrium gap*,  $\Delta \bar{x}_i$ , as the displacement between two vehicles that results in no net acceleration at the start of the simulation (i.e.  $t = 0$ ). Similarly, we define the *final equilibrium gap*,  $\Delta \bar{x}_f$ , as the separation between two vehicles that results in no net acceleration once the system has achieved homogeneity. Note that it is not necessarily true that  $\Delta \bar{x}_i = \Delta \bar{x}_f$  as the system may not be homogeneous at  $t = 0$  and therefore may have a different initial equilibrium gap (see Fig. 2).

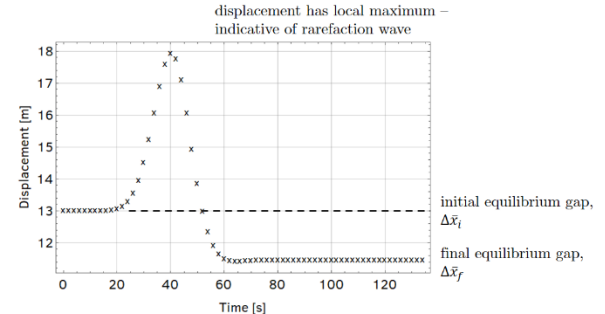


Figure 2<sup>[3]</sup>: Plot showing the displacement against time for a single vehicle in a rarefaction wave.

Since  $\Delta \bar{x}_f$  is defined exclusively in the homogeneous case, we may find an analytic expression for  $\Delta \bar{x}_f$  by noting that  $\Delta v_\alpha = 0$  is a condition for homogeneity and setting  $dv_\alpha/dt = 0$  in Eq. (2.1). This yields,

$$\Delta \bar{x}_f = \frac{s_0 + T v}{\sqrt{1 - \left(\frac{v}{v_0}\right)^4}} \quad (2.9)$$

where  $s_0^{(\alpha)} \rightarrow s_0$ ,  $T_\alpha \rightarrow T$ ,  $v_\alpha \rightarrow v$  and  $v_0^{(\alpha)} \rightarrow v_0$  in the homogeneous case.

Then, the equilibrium gap is a function of the final speed of the vehicles. This is important as it characterises the separation that a system will tend to as simulation time  $t \rightarrow \infty$ . In the limit  $v \ll v_0$ , the denominator in Eq. (2.9) is negligible so  $\Delta \bar{x}_f \rightarrow s_0 + T v$ . The reciprocal of the final equilibrium gap,

defined as  $\rho = 1/\Delta\bar{x}_f$ , is analogous to the density of vehicles.

For a system of  $N$  vehicles, consider plotting the displacement of every vehicle against time. Then, consider curve-fitting a function,  $p(t)$ , to the stationary points of the displacement-time curve for each vehicle. The function  $p(t)$  now gives a time-continuous description of the maximum

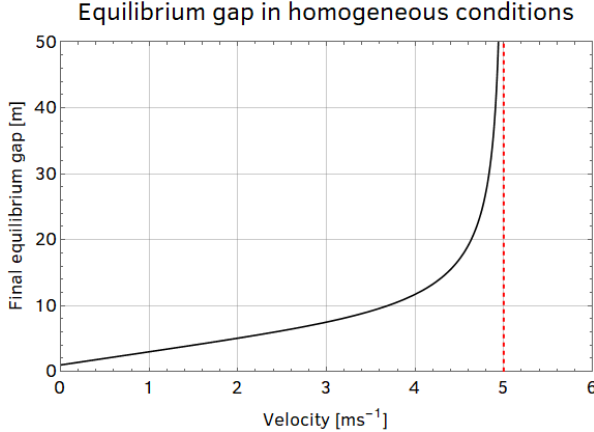


Figure 3<sup>[3]</sup>: Plot of Eq. (2.9) showing how the final equilibrium gap changes with velocity for fixed  $s_0 = 1\text{m}$ ,  $T = 2\text{s}$  and  $v_0 = 5\text{ms}^{-1}$  (solid line). The final equilibrium gap tends to an asymptote at  $v = v_0$  (dashed line).

displacement (for rarefaction waves) or minimum displacement (for compression waves). We define the *amplitude* of the wave,  $A(t)$ , as,

$$A(t) = p(t) - \Delta\bar{x} \quad (2.10)$$

where  $\Delta\bar{x} = \max\{\Delta\bar{x}_i, \Delta\bar{x}_f\}$  for a rarefaction wave and  $\Delta\bar{x} = \min\{\Delta\bar{x}_i, \Delta\bar{x}_f\}$  for a compression wave. This ensures that the magnitude of the amplitude  $|A(t)| = |p(t) - \Delta\bar{x}|$  takes the smallest value.

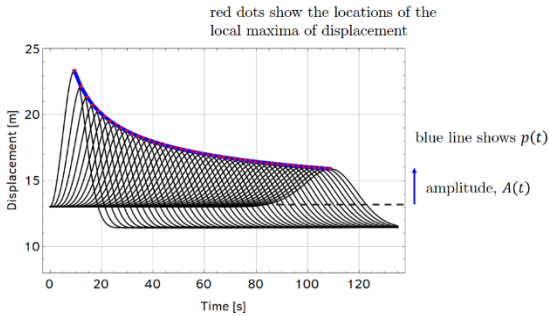


Figure 4<sup>[3]</sup>: Plot showing the displacement against time for a rarefaction wave. The red points represent the local maxima of displacement for each vehicle and the blue line connecting these points is  $p(t)$ . Then, the amplitude is  $A(t) = p(t) - \Delta\bar{x}$  where  $\Delta\bar{x} = \max\{\Delta\bar{x}_i, \Delta\bar{x}_f\} = \Delta\bar{x}_i$  in this case.

By definition, a rarefaction wave has a displacement-time graph whose stationary points correspond to local maxima. Hence,  $A(t) \geq 0$  for rarefaction wave-packets and  $A(t) \leq 0$  for compression wave-packets.

We define the wave speed,  $c(t)$ , as the rate of change of position of the stationary points on the

displacement-time graph of each vehicle. Let  $(t_\alpha, x_\alpha)$  represent the time,  $t_\alpha$ , and position,  $x_\alpha$ , at which the  $\alpha^{\text{th}}$  vehicle attains its stationary point of displacement. Then, plot  $x_\alpha$  against  $t_\alpha$  for each vehicle and let  $C(t)$  be a continuous interpolated function that approximates the points. The wave speed,  $c(t)$ , is given by the time-derivative of  $C(t)$ .

$$c(t) = \frac{dC(t)}{dt} \quad (2.11)$$

Lastly, we define the wavelength,  $\lambda(t)$ , as the full-width at half-maximum of the amplitude peak on a plot of the displacement against the position of each car (see Fig. 5).

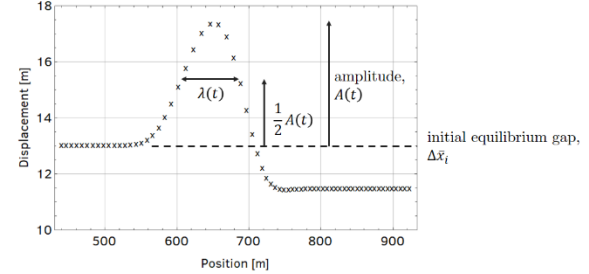


Figure 5<sup>[3]</sup>: Plot showing the displacement against position for a single vehicle in a rarefaction wave. The wavelength of the wave is the full-width at half-maximum of the amplitude peak.

### III. PROGRAMMING

#### A. Programming Language

In order to produce a visual animation of the traffic model, we would require a high-level programming language. We also considered weakly-typed and interpreted languages to allow quick development without compilation. We decided to use NodeJS, a Windows-level implementation of the Google Chrome V8 JavaScript interpreter, to produce the animations.

NodeJS was ideal because it has high-level functionality with pre-defined complex mathematical functions, which are useful in numerical integration. Unlike JavaScript, NodeJS has access to the file-system, so can be used for creating and reading from locally-stored databases. The syntax for NodeJS is identical to JavaScript, which offers native support for rendering graphics. Finally, NodeJS natively supports JavaScript Object Notation (JSON) files, which is a popular data-storage format that is convenient for complex datasets.

For data analysis, we used both Python and Mathematica to produce and extract data from plots. Python is an open-source, flexible language that offers a range of modules for data analytics and producing professional plots. Mathematica is proprietary software which has very high-level functionality for complex data analytics and

vectorisation operations for fast data manipulation. Mathematica offers native JSON support while Python provides JSON functionality through a library.

### B. Numerical Integration Method

The simplest and least computationally-intensive method for finding numerical solutions of an ordinary differential equation is the Euler method. However, the Euler method can be unstable when the system is oscillatory<sup>[5]</sup>, as in the case of traffic waves.

Instead, we consider the Runge-Kutta family of methods, which can be stable for oscillatory systems if the step size is sufficiently small. We take the fourth-order Runge-Kutta method (RK4) to solve the IDM system which offers an optimal compromise between accuracy and speed (see Table II).

Table II<sup>[5]</sup>: A comparison of the Runge-Kutta family of methods, with the steps needed per time-step,  $\Delta t$ , and the cumulative error of the  $N^{\text{th}}$  order Runge-Kutta method. Note that the fifth-order method offers no improvement on the order of the error compared to the fourth-order method, so we choose to use RK4.

Order	3	4	5	6	7
Steps	3	4	5	6	7
Error	$O(\Delta t^3)$	$O(\Delta t^4)$	$O(\Delta t^4)$	$O(\Delta t^5)$	$O(\Delta t^6)$

There are a number of modules available that implement RK4 in NodeJS, but here we choose to program a custom, minimal implementation for efficiency. To use RK4 to solve the second-order differential equation in Eq. (2.1), we parameterise the system as 2 first-order ordinary differential equations,

$$\frac{dx_\alpha}{dt} = v_\alpha \quad (3.1)$$

$$\frac{dv_\alpha}{dt} = a_\alpha \left[ 1 - \left( \frac{v_\alpha}{v_0^{(\alpha)}} \right)^4 - \left( \frac{s^*(v_\alpha, \Delta v_\alpha)}{\Delta x_\alpha} \right)^2 \right] \quad (3.2)$$

where each of the parameters is defined as previously.

For a differential equation of the form  $dy/dt = f(t, y)$  and given an initial condition  $y(t_0) = y_0$ , the four intermediate steps of the RK4 method for the  $n^{\text{th}}$  time-step are<sup>[5]</sup>,

$$\begin{aligned} k_1 &= \Delta t \cdot f(t_n, y_n) \\ k_2 &= \Delta t \cdot f(t_n + \Delta t/2, y_n + k_1/2) \\ k_3 &= \Delta t \cdot f(t_n + \Delta t/2, y_n + k_2/2) \\ k_4 &= \Delta t \cdot f(t_n + \Delta t, y_n + k_3) \end{aligned} \quad (3.3)$$

where  $\Delta t$  is the time-step. The new values of  $t_n$  and  $y_n$  are,

$$\begin{aligned} t_{n+1} &= t_n + \Delta t \\ y_{n+1} &= y_n + (k_1 + 2k_2 + 2k_3 + k_4)/6 \end{aligned} \quad (3.4)$$

where  $y_{n+1}$  is calculated using a weighted average of the intermediate steps  $k_1$ ,  $k_2$ ,  $k_3$  and  $k_4$ .

### C. Testing

A number of programming techniques were used to test the software during and after development.

The software was written as a modular program using object-oriented programming. Therefore, each module could be unit-tested individually and bugs could be traced back easily to the erroneous module.

Rendering each scenario as an animation prior to outputting data meant we could quickly check to verify that the scenario was behaving as expected without carrying out any data analysis.

To verify that the simulation was correct, we compared the results to the theoretical predictions made in Section II, C. For example, we considered how the final equilibrium gap changed with velocity (see Fig. 6) to verify if Eq. (2.9) holds. Testing based on individual vehicle behaviour is discussed in more detail in Section IV, A.

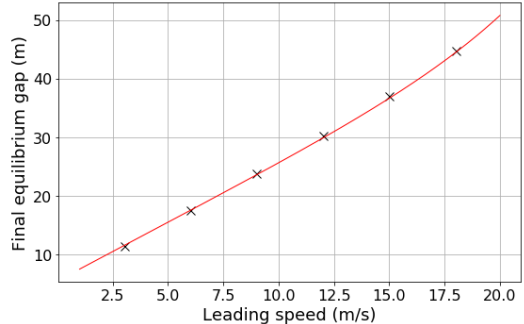


Figure 6<sup>[6]</sup>: Plot showing how the final equilibrium gap changes with the speed of the leading vehicle. The relationship described in Eq. (2.9) is also shown (red line). The standard error of sample means is  $\sigma = 0.3\text{m}$  which is small relative to the length scale of the final equilibrium gap ( $\sim 30\text{m}$ ) so the simulation strongly agrees with the theoretical prediction.

Parameter testing was used to ensure the system behaved as expected. Each parameter was changed individually to ensure the effect was consistent with the behaviour expected from the definition of the parameter. This is discussed further in Section IV, B. During parameter testing, we identified a small sign error in the brief and this was subsequently fixed.

We also used boundary-case testing to check the behaviour of the system for extreme values. For example, we set the desired velocity of a vehicle to 0 to model it as stationary, but discovered that this caused Eq. (2.1) to diverge so virtual vehicles were developed instead.

## IV. RESULTS

### A. Individual Vehicle Behaviour

We verify if individual vehicles are behaving as expected by considering the following two scenarios. In the first scenario, we consider a single vehicle accelerating from rest with a large initial gap as it approaches a traffic light, and then decelerating to a stop. Using standard parameters described in Table III, we consider the acceleration and velocity against time to investigate how the model behaves.

Table III: Standard vehicle parameters. Justification for these values is presented in Section IV, B.

Parameter	Standard Value
$a$	$0.9\text{ms}^{-1}$
$b$	$1.5\text{ms}^{-1}$
$T$	$2.0\text{s}$
$v_0$	$30\text{ms}^{-1}$
$s_0$	$5.0\text{m}$

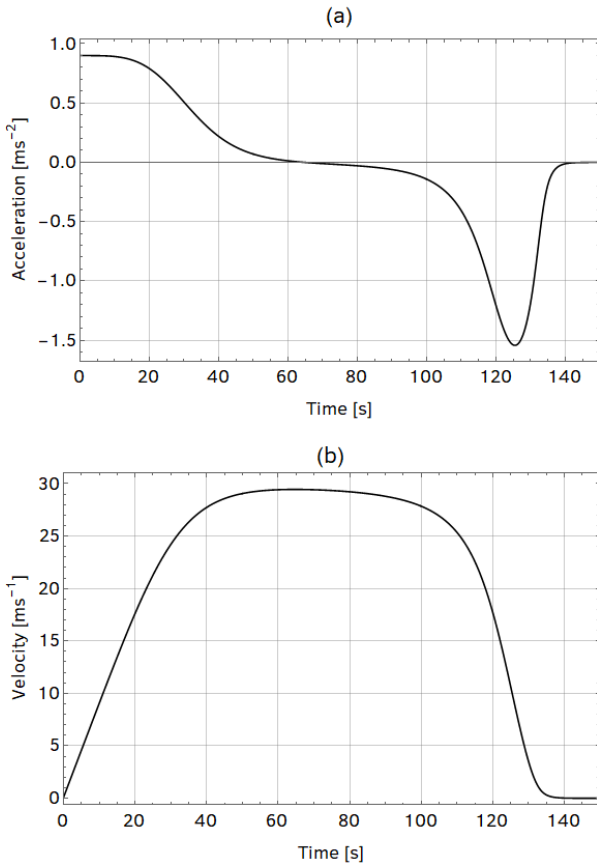


Figure 7<sup>[3]</sup>: Plot showing the acceleration against time (a) and velocity against (b) of a vehicle as it approaches a traffic light from a large gap.

From Fig. 7, we note that the behaviour is as predicted. Initially, the distance to the traffic light is large so the coupling term in Eq. (2.3) is almost negligible and hence the vehicle accelerates as if it was on a free road according to Eq. (2.4), reaching its desired velocity at  $t = 50\text{s}$ . However, as the vehicle approaches the traffic light, the coupling term begins to cause a deceleration, with the vehicle

achieving its peak deceleration of approximately  $b_\alpha = 1.5\text{ms}^{-2}$  at  $t = 126\text{s}$ . The vehicle continues to decelerate until it comes to a rest at  $t = 135\text{s}$  when it has reached the traffic light.

We now investigate the case of a fast moving vehicle with a large initial gap approaching a slow moving vehicle. Using the same parameters as in Table III for the fast-moving vehicle and setting  $v_\alpha = v_0^{(\alpha)} = 10\text{ms}^{-1}$  for the slow-moving vehicle, we see the velocity and displacement of the vehicles in Fig. 8.

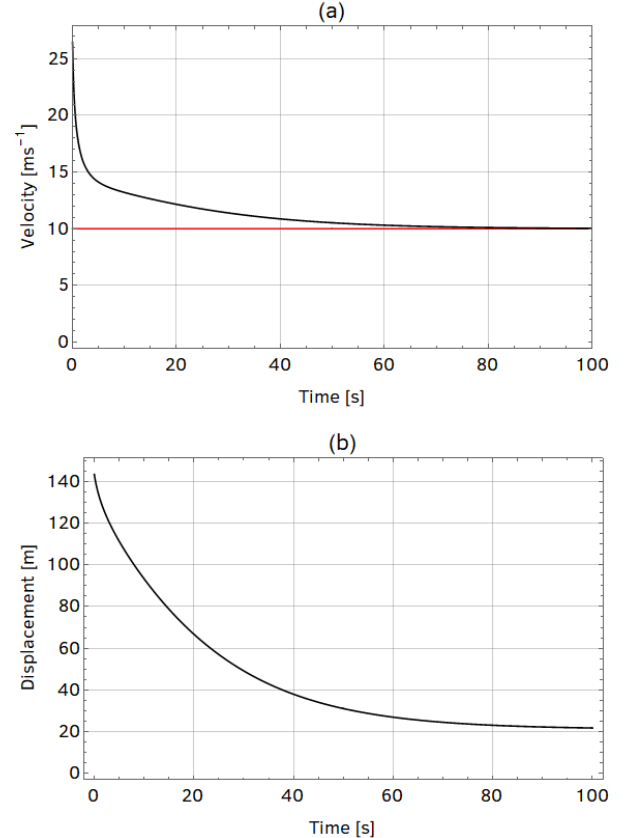


Figure 8<sup>[3]</sup>: Plots showing the velocities against time (a) of the slow, leading vehicle (red line) and fast, trailing vehicle (black line) and displacement against time (b) of the trailing vehicle as it approaches the leading slower vehicle.

Fig. 8 also shows the expected behaviour. As the trailing vehicle approaches the slower, leading vehicle, their velocities tend to the same value and the IDM equation reduces to a vehicle-following algorithm with the speed of the trailing vehicle limited by the speed of the leading vehicle  $v_\alpha = 10\text{ms}^{-1}$ . As simulation time  $t \rightarrow \infty$ , the final equilibrium gap tends to  $\Delta\bar{x}_f \approx 21\text{m}$ , which agrees with the predicted result from Eq. (2.9).

By conducting these individual vehicle scenarios, we have verified that the simulation is producing the expected results.

### B. Parameter Testing

Now, let us justify the standard parameter values stated in Table III. The desired velocity,  $v_0 =$

$30\text{ms}^{-1} \approx 70\text{mph}$ , is the legal motorway speed and provides an upper-limit to the desired velocity. The jam distance,  $s_0 = 5.0\text{m}$ , is the sum of the length of a typical car,  $l \approx 4.5\text{m}$ , and a small physical gap between vehicles of around 50cm.

To justify the values for the safe-time headway, maximum acceleration and desired deceleration, we consider the effect of changing these parameters on the acceleration of the vehicle in the scenario of a vehicle approaching a traffic light from a large initial gap.

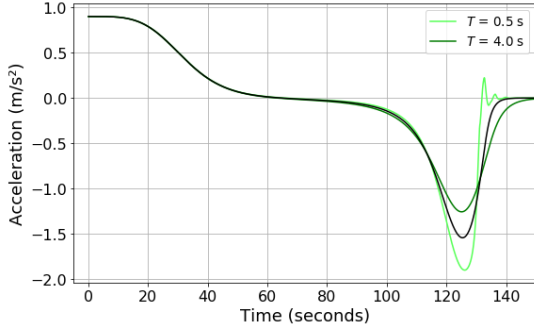


Figure 9<sup>[6]</sup>: Plot showing the effect of using safe-time headway values of  $T = 0.5\text{s}$  (light green line) and  $T = 4.0\text{s}$  (dark green line) on the acceleration of a vehicle approaching a traffic light from a large distance. The acceleration of the vehicle with standard parameter  $T = 2.0\text{s}$  (black line) is also shown.

In Fig. 9, we note that the safe-time headway has a negligible effect on the initial acceleration of each vehicle. A larger value for  $T$  appears to cause the vehicle to begin decelerating earlier, which results in a small peak deceleration that is less than the desired deceleration. This appears to be consistent with the behaviour of careful drivers, who are more likely to decelerate earlier and more gently when encountering a change in traffic conditions. The opposite is true for  $T = 0.5\text{s}$ .

In the case for  $T = 0.5\text{s}$ , the acceleration oscillates about  $\frac{dv}{dt} = 0$  at  $t = 130\text{s}$ . The oscillation occurs because a lower value for  $T$  causes the driver to react more impulsively. This results in the driver overshooting the desired deceleration and then compensating by inducing an oscillation about the target acceleration. In the real world, this type of oscillation of the acceleration is unrealistic and therefore values of  $T < 1.0\text{s}$  should not be used for the simulation. We take  $T = 2.0\text{s}$  as the standard value because this is the value at which the peak deceleration is approximately equal to the desired deceleration.

First, we consider the effect of changing the maximum acceleration,  $a$ . For  $a = 3.0\text{ms}^{-2}$ , the driver quickly accelerates to the desired velocity by  $t = 25\text{s}$  and then quickly decelerates to halt by  $t = 120\text{s}$ . For  $a = 0.3\text{ms}^{-2}$ , the driver does not stop accelerating until  $t = 125\text{s}$  and then comes to a halt by  $t = 180\text{s}$ . Evidently, with lower values of  $a$ , the reaction of a driver to a change in traffic conditions is less effective and therefore is more likely to induce

multiple traffic waves. Taking  $a = 0.9\text{ms}^{-2}$  allows us to induce singular traffic wave-packets. In some investigations, we may choose to lower the maximum acceleration to induce more complex vehicle behaviour.

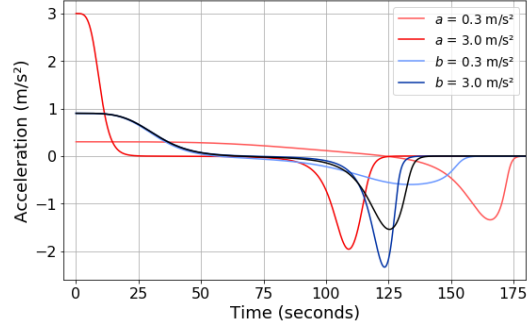


Figure 10<sup>[6]</sup>: Plot showing the effect of using maximum acceleration values of  $a = 0.3\text{ms}^{-2}$  (pink line),  $a = 3.0\text{ms}^{-2}$  (red line), and desired acceleration values of  $b = 0.3\text{ms}^{-2}$  (blue line),  $b = 3.0\text{ms}^{-2}$  (dark blue line) on the acceleration of a vehicle approaching a traffic light from a large distance. The acceleration of a vehicle with standard values is also shown (black line). For each change in variable, the other variables are fixed according to the standard parameters in Table III.

Using higher values for the desired deceleration allows a vehicle to start decelerating later. With  $b = 0.3\text{ms}^{-2}$ , the vehicle begins its deceleration at  $t = 65\text{s}$  and continues to decelerate for  $\Delta t = 95\text{s}$ . Meanwhile, for  $b = 3.0\text{ms}^{-2}$ , the vehicle begins to decelerate at  $t = 85\text{s}$  and stops decelerating after  $\Delta t = 45\text{s}$ . Setting a low value for the desired deceleration is consistent with the behaviour of careful drivers while the opposite is true for aggressive drivers. We take  $b = 1.5\text{ms}^{-2}$  as a balance between the behaviour of a careful and aggressive driver.

Note that  $b > a$  in the standard values because  $b$  is a deceleration and hence is limited by the braking ability of the vehicle rather than the power generated by the engine. A vehicle is easily capable of accelerating faster than  $a = 0.9\text{ms}^{-2}$ , but this value was chosen as it was more suitable for producing traffic waves in slow-moving traffic.

### C. Standard Compression Wave

We can induce a compression traffic wave by simulating a scenario which produces an area of high local vehicle density. For example, consider the scenario of vehicles travelling homogeneously at their desired speed of  $v_0^{(a)} = 3\text{ms}^{-1}$  with displacements equal to the initial equilibrium gap. Let the leading vehicle be momentarily at rest, such that the trailing vehicles create an area of high local density as they approach the stationary vehicle (see Fig. 11). After a small finite time, let the first vehicle begin to accelerate to its desired speed. Then, the displacement-time graph for this scenario is shown in Fig. 12.

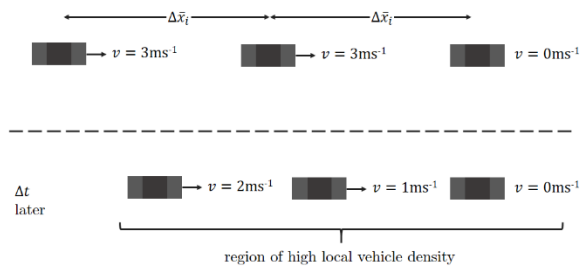


Figure 11<sup>[3]</sup>: Inducing a compression wave.

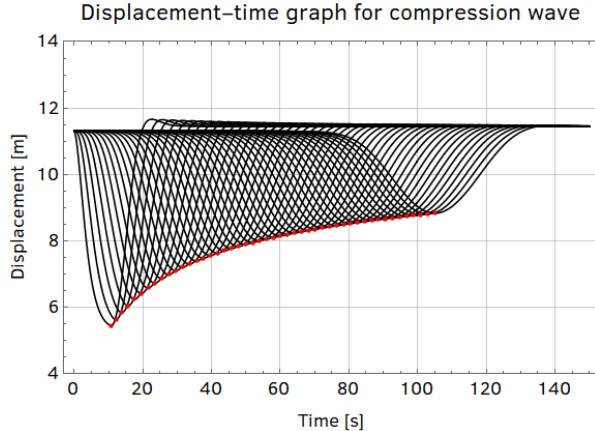


Figure 12<sup>[3]</sup>: Plot showing the displacement against time for a system of  $N = 50$  vehicles with a standard compression wave scenario. The red points indicate the points of local minimum displacement for each vehicle.

An interesting feature of Fig. 12 is the oscillation about the equilibrium position at approximately  $t = 20$ s. This occurs because the standard parameters we have used for the vehicles cause the driver to overshoot the target displacement, which is the final equilibrium gap,  $\Delta\bar{x}_f \approx 11.5$ m. While it is possible to find values for parameters that will lead to a critically-damped system for a given scenario, often most systems will undergo some oscillation about the target value.

For example, consider the mechanism in a proportional-integral-derivative (PID) controller, which is used in real-time systems such as the autopilot in an aircraft. The controller uses parameters  $K_p$ ,  $K_i$  and  $K_d$  which are coefficients for each of the three terms in the PID controller. Usually, the parameters do not lead to a critically damped system and often an aircraft will carry out damped oscillations about a reference value (e.g. the aircraft may oscillate about a given altitude set in the autopilot). This process is shown in Fig. 13.

By plotting the position of each vehicle against the time at which it achieves its minimum displacement, we can obtain Fig. 14.

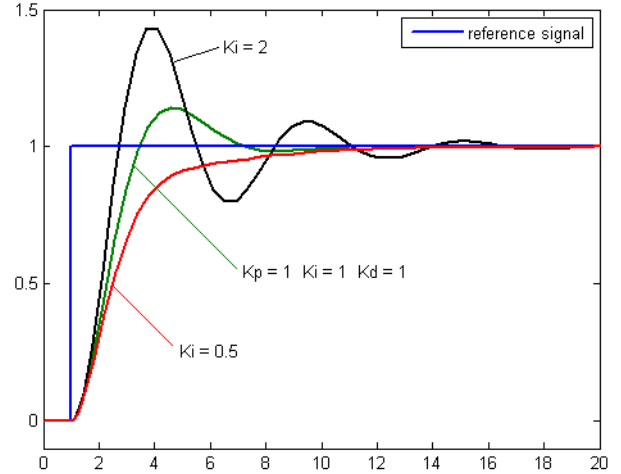


Figure 13<sup>[7]</sup>: For fixed coefficients  $K_p = 1$  and  $K_d = 1$  for the proportional and derivative terms in a PID controller, different values of  $K_i$  can lead to under-damped (black line, green line), critically-damped or over-damped (red line) scenarios. In the under-damped case, there is some oscillation about the reference signal.

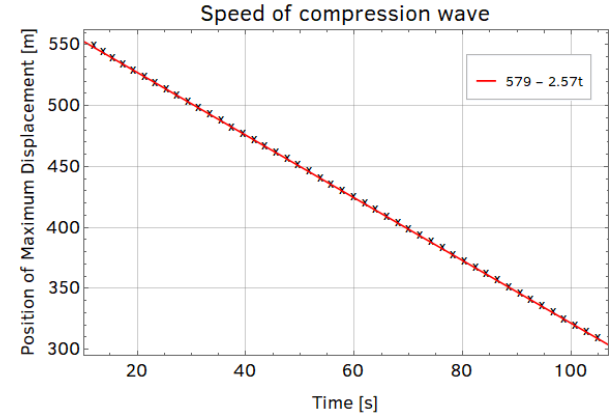


Figure 14<sup>[3]</sup>: A plot of the position of each vehicle against the time at which it attains its minimum displacement in a compression wave.

From the gradient of Fig. 14, we calculate the speed of the compression wave as  $dC/dt = (-2.57 \pm 0.01)\text{ms}^{-1}$ . A plot of the absolute amplitude of the compression wave-packet against time is shown in Fig. 15 along with its equivalent log-log graph.

For large  $t$ , the absolute amplitude decays as a power law of  $t^{-0.392}$ . Then, we may write  $|A(t)| = \beta + \gamma t^{-0.392}$  where  $\beta = (7.75 \pm 3.57) \times 10^{-2}$  and  $\gamma = (15.3 \pm 0.2)$  are good approximations for the power law relationship. Note that we use the absolute amplitude because this is a compression wave so  $A(t) < 0$  and hence  $\log A(t)$  is imaginary.

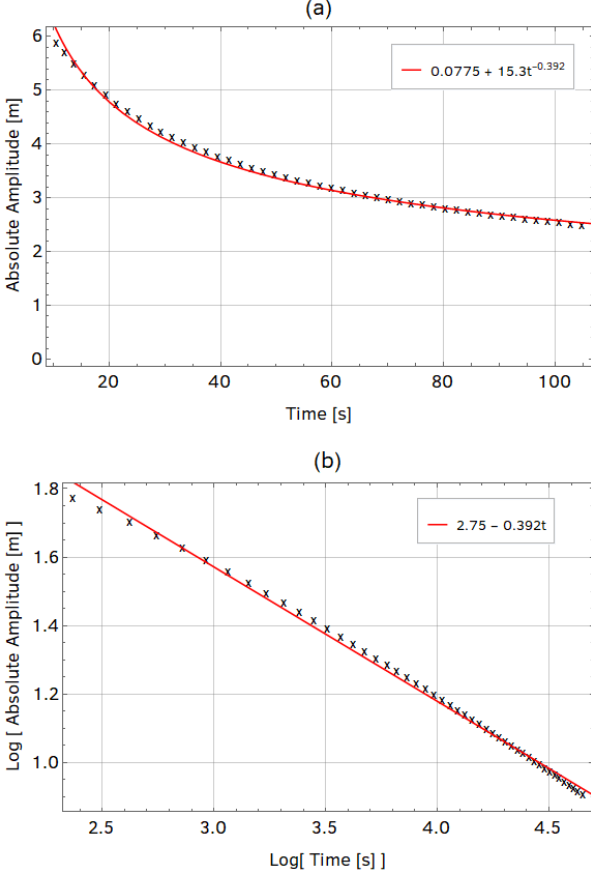


Figure 15<sup>[3]</sup>: Plot showing the absolute amplitude against time (a) and log absolute amplitude against log time (b) of a system of  $N = 50$  vehicles with a standard compression wave scenario.

In Fig. 16, we consider how the wavelength of the compression wave-packet changes with time. Similarly, for large  $t$ , there is a strong indication that the wavelength increases as a power law of  $t^{0.365}$ . Then, the wavelength can be written as  $\lambda(t) = \beta + \gamma t^{0.365}$  with  $\beta = (-0.402 \pm 0.175)$  and  $\gamma = (5.01 \pm 0.04)$ .

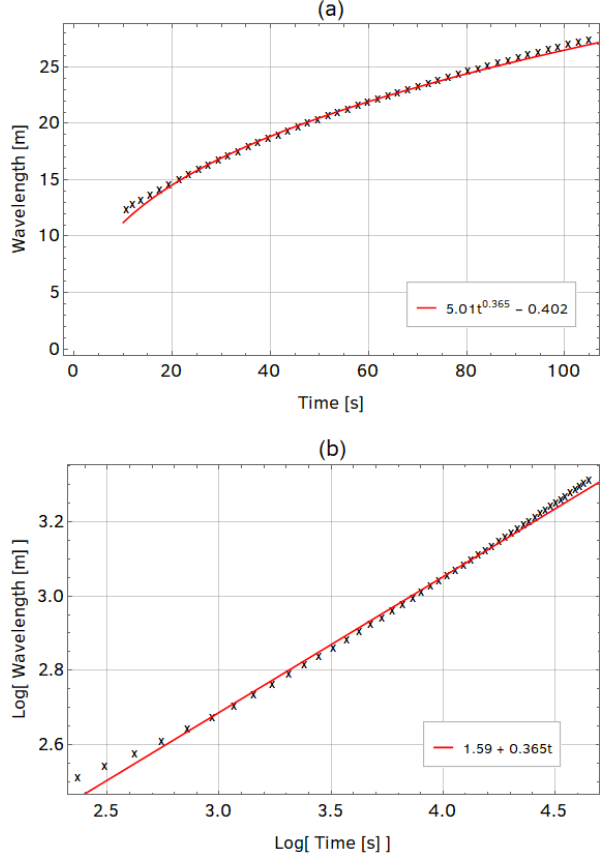


Figure 16<sup>[3]</sup>: Plot showing the wavelength against time (a) and log wavelength against log time (b) of a system of  $N = 50$  vehicles with a standard compression wave scenario.

#### D. Standard Rarefaction Wave

A rarefaction wave is the propagation of an area of low local vehicle density through space. This can be induced using the standard homogeneous conditions for all vehicles as specified in Table III with the additional constraints that all vehicles are separated by the initial equilibrium gap and travel at a speed of  $v_\alpha = 3\text{ms}^{-1}$ . The front vehicle leads by a distance larger than the equilibrium gap but has a fixed desired velocity  $v_0^{(\alpha)} = 3\text{ms}^{-1}$  (i.e. the leading vehicle travels at a constant velocity throughout). The leading initial gap is arbitrary, but  $\Delta x_\alpha = 50\text{m}$  produces a rarefaction wave with an appreciable amplitude (see Fig. 17).

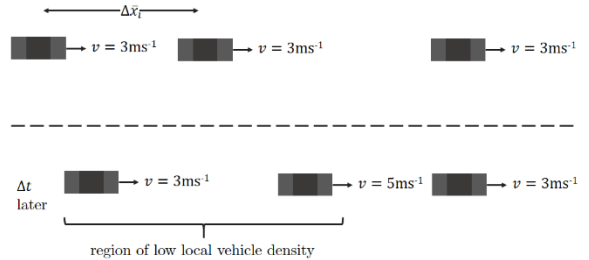


Figure 17<sup>[3]</sup>: Inducing a rarefaction wave.

Fig. 18 shows the position and displacement for each vehicle against time using a system of  $N = 50$  vehicles.

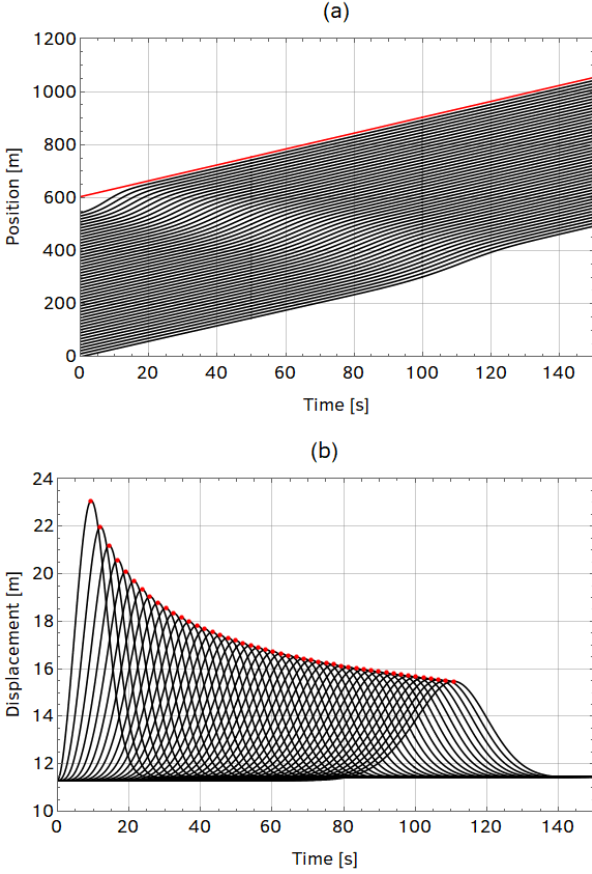


Figure 18<sup>[3]</sup>: Plot showing the position (a) and displacement (b) of a system of  $N = 50$  vehicles with a standard rarefaction wave scenario. The red line in the position plot indicates the trajectory of the leading vehicle. The red points in the displacement plot indicate the points of local maximum displacement for each vehicle, which is used to find the amplitude of the wave.

A rarefaction wave occurs because the initial gap to the leading vehicle is larger than the equilibrium gap and hence the trailing vehicles accelerate sequentially, causing the initial large displacement to propagate backwards through space. By plotting the maximum displacement of each vehicle against the position of the vehicle, we obtain Fig. 19.

The gradient of the plot in Fig. 19 is  $dC/dt = (-2.44 \pm 0.01)\text{ms}^{-1}$ , which we define as the speed of the rarefaction wave. This is different to the wave speed calculated for the compression wave in Section IV, C. The plot appears to show that the wave speed is not constant and increases in magnitude with time, but we approximate the wave speed as linear in the given interval. To verify the behaviour of the wave speed for longer intervals, we consider the same scenario with  $N = 250$  vehicles (see Fig. 20).

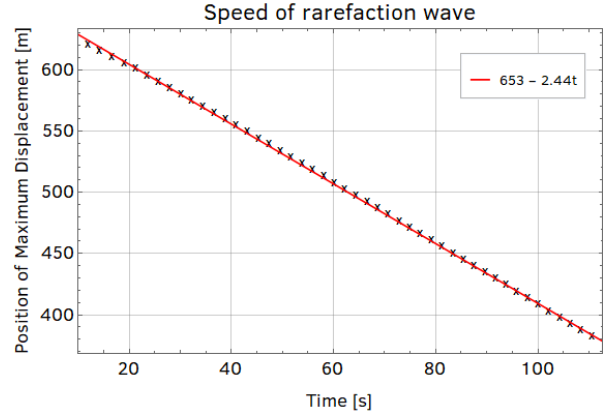


Figure 19<sup>[3]</sup>: Plot showing the position and time at which each vehicle attains its maximum displacement for a system of  $N = 50$  vehicles.

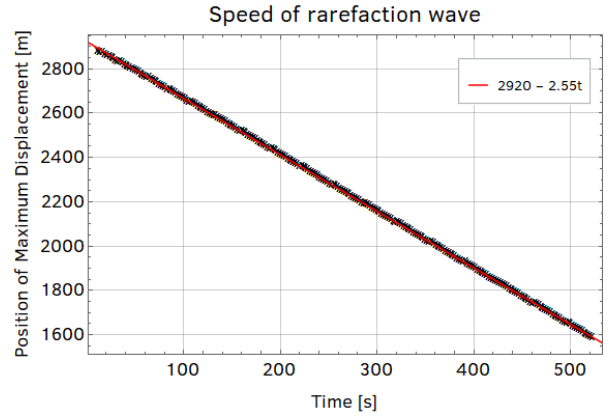


Figure 20<sup>[3]</sup>: Plot showing the position and time at which each vehicle attains its maximum displacement for a system of  $N = 250$  vehicles.

The wave speed,  $dC/dt = (-2.55 \pm 0.01)\text{ms}^{-1}$ , for  $N = 250$  vehicles is greater than the equivalent scenario for  $N = 50$  vehicles but there appears to be no evidence to suggest that the wave speed deviates from linearity for long simulation times. This wave speed is approximately equal to the wave speed of the compression wave calculated in Section IV, C. The wave speed calculated for the  $N = 50$  vehicles scenario is likely to be lower due to statistical noise.

For the  $N = 50$  vehicles system, Fig. 21 shows the amplitude of the rarefaction wave, which is found by plotting the red points in Fig. 18 (b).

From Fig. 21 (b), there is a strong suggestion that the amplitude decays as a power law with time, with the power of  $t$  being approximately equal to  $-0.432$ . Then, fitting a function of the form  $A(t) = \beta + \gamma t^{-0.432}$  on the amplitude curve in Fig. 21 (a) shows the curve is well approximated by  $\beta = (2.59 \pm 1.02) \times 10^{-2}$  and  $\gamma = (30.8 \pm 0.1)$ .

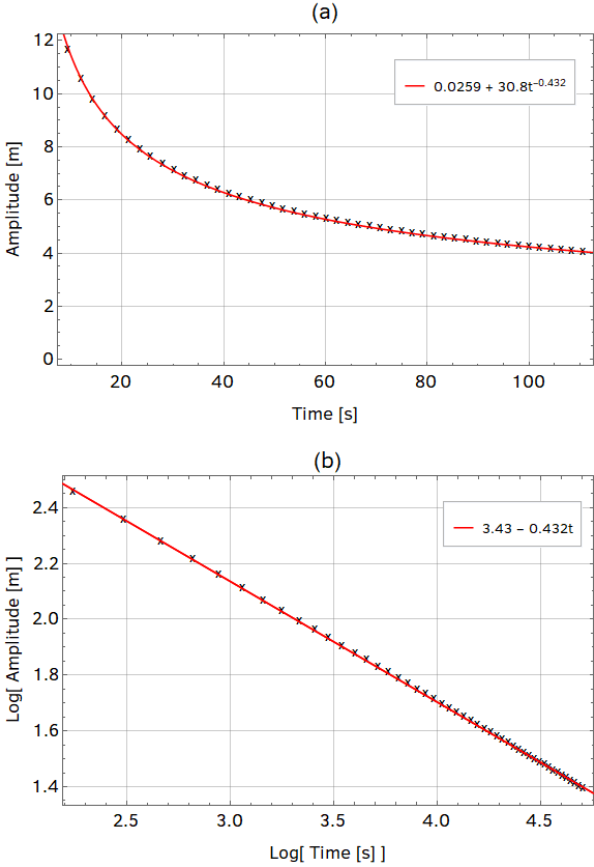


Figure 21<sup>[3]</sup>: Plot showing the amplitude against time (a) and log amplitude against log time (b).

We can also calculate the wavelength of the wave-packet and analyse how it disperses over time, as shown in Fig. 22.

While there is some deviation from the line of linear regression in Fig. 22 (b) for small  $t$ , the general trend is approximately linear. The wavelength can then be written as  $\lambda(t) = \beta + \gamma t^{0.381}$  with  $\beta = (-1.03 \pm 0.11)$  and  $\gamma = (4.07 \pm 0.02)$ . Note that as the amplitude of the wave decreases, the wavelength increases so the wave-packet is dispersing.

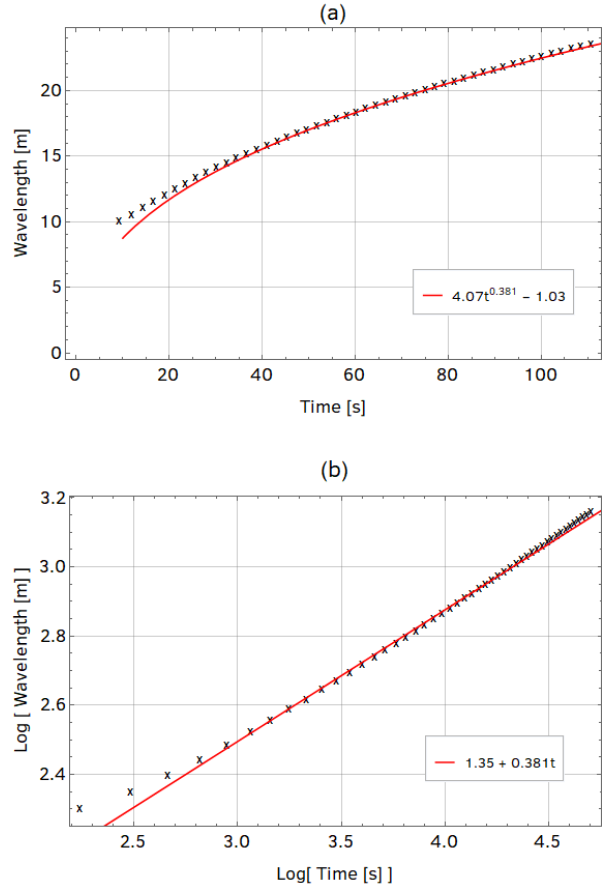


Figure 22<sup>[3]</sup>: Plot showing the wavelength against time (a) and log wavelength against log time (b) for  $N = 50$  vehicles. This was used to verify that the wavelength of the wave increased as a power law.

#### E. Inducing Semi-Stable and Unstable Behaviour

For this section, we will analyse just the standard rarefaction wave but the analysis is identical for a compression wave. We will investigate the effect of changing the maximum acceleration to induce semi-stable and unstable behaviour. We have seen from Fig. 18 (a) that a value of  $a_\alpha = 0.9\text{ms}^{-2}$  produces a stable system where a single rarefaction wave-packet propagates through space. However, reducing the value of the maximum acceleration to  $a_\alpha = 0.3\text{ms}^{-2}$  causes a semi-stable state where the initial rarefaction wave induces multiple secondary and tertiary compression and rarefaction waves, as shown in Fig. 23.

The displacement plot in Fig. 23 (b) shows that initially a rarefaction wave is induced in the normal way. However, the system does not tend to stability immediately and initially overshoots the final equilibrium gap at  $t = 30\text{s}$ . The first vehicle corrects for this by decelerating, but again overshoots the target displacement at  $t = 50\text{s}$ . This oscillation about the final equilibrium gap induces further compression and rarefaction waves.

The value of the maximum acceleration appears to limit the receptiveness of the driver to the behaviour of the vehicle ahead. This causes the

overshooting behaviour described in Fig. 23 and is the reason for multiple waves being induced. Fig. 24 shows the velocity-time plot the for scenario above.

In Fig. 24, multiple traffic waves also cause the velocity of the vehicles to oscillate about the final equilibrium velocity,  $\bar{v}_f = 3.0\text{ms}^{-1}$ . This is known as *stop-and-go* traffic and results in an inefficient use of the road since the traffic wave persists for a long time. We discuss the wider implications of this in Section V, B.

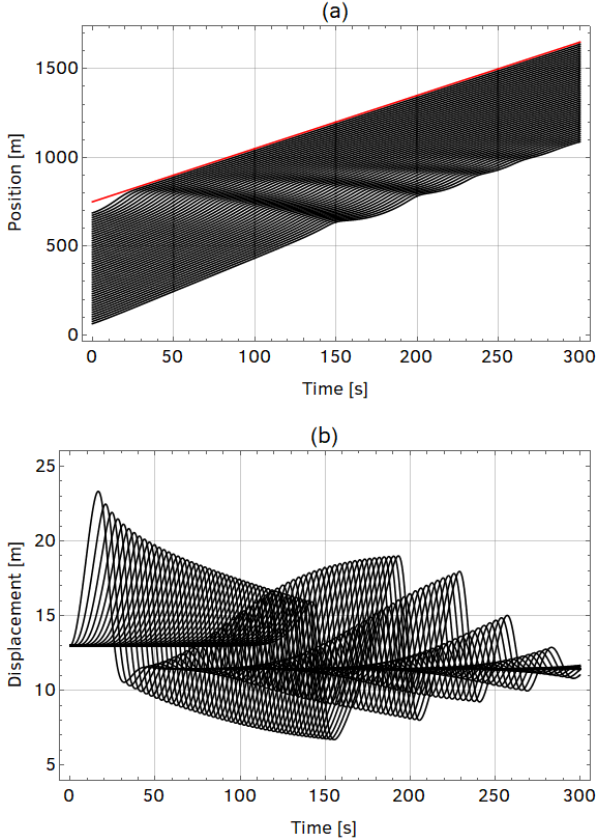


Figure 23<sup>[3]</sup>: Plot showing the position against time (a) and displacement against time (b) for a standard rarefaction wave with  $a_\alpha = 0.3\text{ms}^{-2}$ . In the position plot, the trajectory of the leading vehicle is shown in red. Note the multiple rarefaction and compression waves in the position plot, which correspond to the maxima and minima on the displacement plot, respectively.

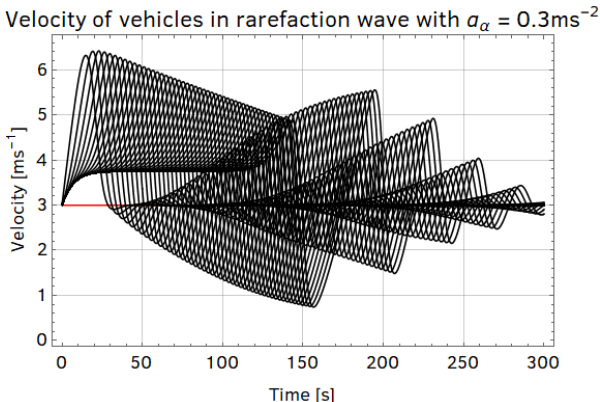


Figure 24<sup>[3]</sup>: Plot showing the velocity against time for a standard rarefaction wave with  $a_\alpha = 0.3\text{ms}^{-2}$ . The velocity of the leading vehicle is shown in red.

Reducing the value of the maximum acceleration further to  $a_\alpha = 0.1\text{ms}^{-2}$  causes the IDM equation to become unstable and diverge, as shown in Fig. 25.

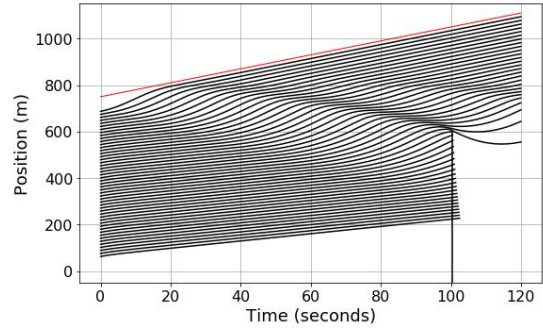


Figure 25<sup>[3]</sup>: Plot showing the position against time for a standard rarefaction wave with  $a_\alpha = 0.1\text{ms}^{-2}$ . The trajectory of the leading vehicle is shown in red.

From Fig. 25, the instability occurs at  $t = 100\text{s}$  when the compression wave induced by the initial rarefaction wave causes the displacement to reduce to less than the desired minimum gap, so  $\Delta x_\alpha \ll s^*$ . This leads to an unbounded negative acceleration as predicted in Section II, B.

#### F. Inhomogeneous Conditions

The system can also be configured to simulate inhomogeneous conditions. This is a more realistic scenario where each driver abides by different parameter values. However, the results from this investigation are relatively uninteresting because the overall behaviour of the system is then dictated by the vehicles which have the most extreme values. Consider a scenario of  $N$  vehicles each with different desired velocities. Then, the vehicle with the slowest desired velocity will limit the velocity of all trailing vehicles.

As an example, we take the scenario of the standard rarefaction wave but each  $N = \{11, 21, 31, 41\}$  vehicle is a truck with  $a_\alpha = 0.3\text{ms}^{-2}$  and  $s_0^{(\alpha)} = 20\text{m}$ . Then, the speed of each vehicle against time is shown in Fig. 26.

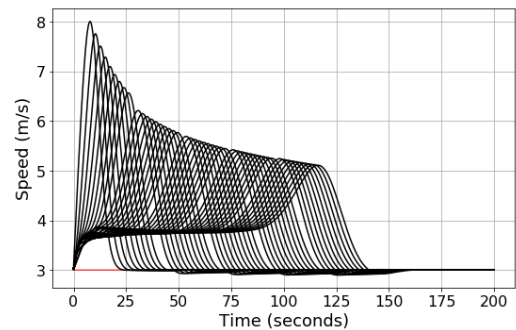


Figure 26<sup>[6]</sup>: Plot showing the speed against time for a standard rarefaction wave. Each  $N = \{11, 21, 31, 41\}$  vehicle is a truck with  $a_\alpha = 0.3\text{ms}^{-2}$ . The trajectory of the leading vehicle is shown in red.

In Fig. 26, although the trucks accelerate slower than the other vehicles, the general trend is as observed in Section IV, D. The analysis of the rarefaction wave produced in this scenario is more difficult since the trucks have different  $s_0^{(\alpha)}$  values to the other vehicles and hence have different final equilibrium gaps according to Eq. (2.9). Note the oscillation of the speed of the truck about the final equilibrium speed at  $t = 50\text{s}$ . A lower value of  $a_\alpha$  induces oscillations about the target speed, analogous to the behaviour of a PID controller as explained in Section IV, C.

## V. DISCUSSION

### A. Compression and Rarefaction Waves

We have already discussed the results from the analysis of compression and rarefaction waves. We note that for the compression wave, the wave speed was calculated as  $dC/dt = (-2.57 \pm 0.01)\text{ms}^{-1}$  with  $N = 50$  vehicles. The wave speed was  $dC/dt = (-2.55 \pm 0.01)\text{ms}^{-1}$  for  $N = 250$  vehicles for the standard rarefaction wave. Therefore, for standard parameters, the wave speed is the same for both compression and rarefaction waves. This agrees with our understanding of waves because the speed of a wave is dependent on the properties of the medium through which it propagates. Since the vehicle parameters are the unchanged in both scenarios, the ‘medium’ is the same.

We note that the amplitude of both the rarefaction and compression waves decays as a power law with  $|A(t)| \sim t^{-0.4}$ . Equally, the wavelength increases as  $\lambda(t) \sim t^{0.4}$  for both types of wave-packets. This describes an approximate dispersion relation for the wave-packets. The implications of this will be discussed further in Section VI.

### B. Semi-Stable and Unstable Behaviour

We discussed how the behaviour of the IDM equation can be made semi-stable and unstable by changing the maximum acceleration parameter in Section V, E. We noted that the system was stable and produced singular, isolated and localised wave-packets for  $a_\alpha = 0.9\text{ms}^{-2}$ , but that reducing the maximum acceleration caused the system to become less stable. In particular,  $a_\alpha = 0.3\text{ms}^{-2}$  gave rise to stop-and-go traffic and  $a_\alpha = 0.1\text{ms}^{-2}$  caused divergence in the IDM equation.

The maximum acceleration parameter characterises the extent to which a vehicle can react to a disturbance in the displacement from its equilibrium displacement. The vehicle acceleration described in Eq. (2.1) is a multiple of the maximum acceleration parameter. Therefore, reducing the value of  $a_\alpha$  also limits the vehicle acceleration and deceleration, causing the driver to overshoot its target equilibrium displacement. In real-life, this is

equivalent to a tired driver who is not able to maintain a constant equilibrium separation.

The stop-and-go behaviour described above induces multiple traffic waves, which causes the trailing vehicles to also accelerate and decelerate. Therefore, the initial traffic wave-packet causes a disturbance which persists for a longer time. The repeated acceleration and deceleration is fuel-inefficient and can lead to more pollution. Hence, by minimising the number of tired drivers on the road, the effects of stop-and-go traffic can be reduced. An extension to this project would seek to investigate if there is a correlation between tiredness (i.e. receptiveness to road conditions) and stop-and-go traffic in the real world.

### C. Sources of Error

Unlike a laboratory experiment, there is virtually no random error in measurements of the macroscopic properties of the system (e.g. wave speed, wavelength, amplitude, etc.). However, numerically integrating a differential equation introduces an error due to the discretisation of time. As described by Lotkin<sup>[8]</sup>, the error due to the RK4 method is of the order  $O(\Delta t^5)$  in each time-step. Then, for an interval  $T$ , the number of time steps is  $T/\Delta t$  so the cumulative error is of the order  $O(T\Delta t^4)$ . Hence, the error relative to the simulation time is of the order  $O(\Delta t^4)$ . Then, for  $\Delta t = 0.1\text{s}$ , the error due to discretisation of time is negligibly small.

Other sources of error arise from the assumptions within the IDM equation and are more difficult to quantify. For example, the model assumes that on a free-road, a vehicle will accelerate constantly for  $v_\alpha \ll v_0^{(\alpha)}$ . However, all vehicles consist of a transmission system which produces zero acceleration between gear shifts (typically occurring in time of the order  $\Delta t$ ). Therefore, in reality, the integration algorithm should account for these momentary periods of zero acceleration in order to accurately model individual vehicle behaviour.

Even in the inhomogeneous scenario, the IDM model was used to simulate vehicles with parameters that were fixed over time. In reality, drivers will not consistently adhere to a given set of parameters, so a more realistic model would take into account that vehicle parameters may change over time.

In cases where we calculated the wavelength of a wave-packet, it was necessary to use a linear interpolation method to approximate the displacement-position plot to determine the full-width at half-maximum. The error due to the interpolated function is likely to be negligibly small because the time-steps were sufficiently small to accurately approximate the required plot.

## VI. FURTHER INVESTIGATIONS

There are a number of ways in which the findings of this investigation can be developed further. A natural progression would be to modify the setup to model a circular road so that each vehicle is coupled. Then, using standard parameters to induce singular wave-packets (i.e. to prevent interference of multiple wave-packets), it is possible to allow the simulation to run for long periods to determine the behaviour of the wave speed, wavelength and amplitude for large  $t$ . It would be interesting to investigate if the power law relations for the wavelength and amplitude of compression and rarefaction waves persist for long simulation times.

We earlier remarked that the wave speed was constant in the standard rarefaction and compression scenarios because wave speed is dependent on its medium of propagation, which remains the same since the vehicle parameters are unchanged. It would therefore be useful to investigate the effect of changing each parameter on the wave speed. If we are able to find an empirical relation linking each parameter to the wave speed, then it is possible to write the wave speed as a function of the vehicle parameters. Finding these relationships would also offer a deeper insight into the physical effects of each parameter on the behaviour of the wave.

We found a power law relation linking the amplitude and wavelength to time in Section IV, C and Section IV, D. It was clear that the wave-packet disperses in space with time, but we could also investigate how the exponent of  $t$  changes with each of the vehicle parameters. By writing the exponent as a function of the vehicle parameters, we can find the ideal parameters that would maximise the dispersion rate. These results would be useful to the UK Highways Agency, who could use the data to set speed limits so that the traffic wave disperses as soon as possible.

Finally, an extension to the model could allow for multiple lanes to be modelled. For a vehicle in a given lane, the IDM equation could still be used to model the behaviour of the vehicle. However, an additional condition could be applied to allow a driver to decide to change lanes (e.g. a driver travelling at speed  $v_0$  may choose to change lanes if at least three of the vehicles ahead are travelling at speed  $v < v_0$  and if the adjacent lane is moving at speed  $v > v_0$ ). Again, results from this model would be useful to the Highways Agency, who can use the data to decide when it is feasible to use the hard-shoulder as an extra lane on smart motorways.

## REFERENCES

- [1] Lighthill, M. and Whitham, G. (1955). On Kinematic Waves. II. A Theory of Traffic Flow on Long Crowded Roads. *Proceedings of the Royal Society A: Mathematical, Physical and Engineering Sciences*, [online] 229(1178), pp.317-345. Available at: <http://rspa.royalsocietypublishing.org/content/229/1178/317> [Accessed 25 Jun. 2018].
- [2] Phillips, W. (1979). A kinetic model for traffic flow with continuum implications. *Transportation Planning and Technology*, [online] 5(3), pp.131-138. Available at: <https://www.tandfonline.com/doi/abs/10.1080/03081067908717157> [Accessed 25 Jun. 2018].
- [3] Siddiqui, U. (2018). Simulating Traffic Jams. Undergraduate. Imperial College London.
- [4] Ho, D. (2018). Simulating Traffic Jams. PhD. Imperial College London.
- [5] Süli, E. (2014). Numerical Solutions of Ordinary Differential Equations. [online] Oxford: Mathematical Institute, University of Oxford, pp.4-19. Available at: <https://people.maths.ox.ac.uk/suli/nsodes.pdf> [Accessed 25 Jun. 2018].
- [6] Li, M. (2018). Simulating Traffic Jams. Undergraduate. Imperial College London.
- [7] Korkmaz, S. (2007). Change of response of second order system to a step input for varying Ki values.. [image] Available at: [https://upload.wikimedia.org/wikipedia/commons/c/c0/Change\\_with\\_Ki.png](https://upload.wikimedia.org/wikipedia/commons/c/c0/Change_with_Ki.png) [Accessed 25 Jun. 2018].
- [8] Lotkin, M., 1951. On the accuracy of Runge-Kutta's method. *Mathematics of Computation*, 5(35), pp.128-133.